JOURNAL OF Materials CHEMISTRY

Synthesis, crystal structures, and quadratic nonlinear optical properties in a series of push–pull boronate derivatives†

Horacio Reyes,[a] Blanca M. Muñoz,[a] Norberto Farfán,*[a] Rosa Santillan,[a] Susana Rojas-Lima,[b] Pascal G. Lacroix*[c] and Keitaro Nakatani[d]

[a]*Departamento de Química, Centro de Investigación y de Estudios Avanzados de IPN, Apdo. Postal 14-740, 07000 México D. F. E-mail: jfarfan@mail.cinvestav.mx*
[b]*Centro de Investigaciones Químicas, Universidad Autónoma del Estado de Hidalgo, Unidad Universitaria, Carretera Pachuca-Tulancingo Km 4.5, Pachuca, Hidalgo C. P. 42076, México*
[c]*Laboratoire de Chimie de Coordination du CNRS, 205 route de Narbonne, 31077 Toulouse cedex 04, France. E-mail: pascal@lcc-toulouse.fr*
[d]*Laboratoire de Photophysique et Photochimie Supramoléculaires et Macromoléculaires (UMR 8531 du CNRS), Ecole Normale Supérieure de Cachan, Avenue du Président Wilson, 94235 Cachan, France*

Received 31st May 2002, Accepted 23rd July 2002
First published as an Advance Article on the web 30th August 2002

A series of eighteen new 'push–pull' molecules obtained by self-assembly of salicylideniminophenols and various phenylboronic acids is reported. Electric field-induced second-harmonic measurements of the nonlinear optical response reveal that the nature of the phenylboron moieties has a modest influence on the molecular hyperpolarizabilities (β). The crystal data available suggest the possibility of easy rotation of the phenyl substituents, with an energy barrier around 10 kcal mol^{-1}, while a computational investigation conducted at the semi-empirical (INDO) level leads to a prediction of 30% β-modulation occuring upon the rotation.

Introduction

Quadratic nonlinear optical (NLO) materials are playing an increasingly important role in a wide range of photonic applications.[1–3] After the first investigations focused on ferroelectric solids, such as $LiNbO_3$ and KH_2PO_4,[4] the potential NLO interest of organic molecules was recognized in relation to their large molecular hyperpolarizabilities (β) induced by asymmetric charge distribution (donor–acceptor molecules) conjugated through a pathway of π-electrons. Initial research effort has been directed towards finding the strongest donor and acceptor with the longest conjugation length, while the structure of the molecular bridge connecting the two end groups has been rather neglected.[5] However, it was shown that for a pair of donor–acceptor substituents, there is an optimized bridge of given length and nature that maximizes β.[6] These observations gave rise to the idea that the ultimate β optimization has to be conducted at the level of the bridge as well.

More recent years have witnessed a growing interest in molecular-scale devices, in relation to the concept of molecular switches.[7,8] In this context, the incorporation of switchability in NLO materials should lead to various novel applications. However, this has been attempted in only a few instances[9] and, again, much effort has been focused on switching the donor–acceptor strength of the substituents, by proton transfer,[10,11] for instance, or by changing the oxidation state of a metal center involved in a charge transfer process.[12] The possibilities provided by a modulation achieved on the conjugated bridge have not been explored, except in the case of *cis–trans* isomerization of azobenzene chromophores, which leads to β reduction on passing from the *trans* to the *cis* form,[13] and, in the case of bis(3-thienyl)ethene derivatives, in which photocyclization provides efficient NLO switches.[14]

In research aimed at extending the range and properties of conjugated linkers, we report here on a new family of push–pull chromophores, **1** and **2**, summarized in Scheme 1. These compounds derive from the well-known stilbene backbone, to which an arylboron (ArB–) fragment has been added. This family of readily available macrocyclic boron compounds have recently attracted some interest from various perspectives in analytical and supramolecular chemistry.[15–18] Our initial motivation for the present investigations came from our recent observation that the ^{1}H NMR shift of the hydrogen of the imine function (–HC=N–) is influenced by the nature of the ArB– fragment.[19] This behavior suggests that a perturbation induced at the level of ArB– will modulate the electronic features of the bridge and, hopefully, the NLO response.

The present contribution focuses on the synthesis and spectroscopic and NLO properties of compounds **1** and **2**. The crystal structures of **2a**, **2h**, and **2i** are described and used for an INDO (intermediate neglect of differential overlap) analysis of the optical nonlinearities, in conjunction with experimental NLO measurements conducted in solution and in the solid state. In a last section, the effect of the rotation of the ArB– fragment is explored as a possibility for achieving a modulation of the NLO response.

Results and discussion

Synthesis and characterization

In previous studies of compounds containing nitrogen–boron coordination, we have described a series of macrocyclic dimeric compounds obtained by self-assembly of salicylidenimino alcohols and arylboronic acids containing different substituents.[20] In contrast, monomeric compounds are obtained when salicylideniminophenol ligands are reacted with phenylboronic acid.[21]

†Electronic supplementary information (ESI) available: molecular structures of **2h** and **2i**, and experimental synthetic data for **1b**–**1h** and **2b**–**2j**. See http://www.rsc.org/suppdata/jm/b2/b205308j/

 DOI: 10.1039/b205308j

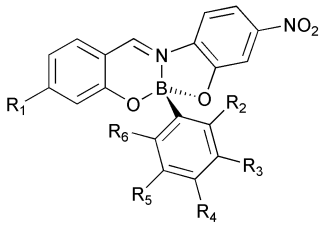

Compounds **1**

R_1	R_2	R_3	R_4	R_5	R_6	
OMe	H	H	H	H	H	*1a*
	H	NO_2	H	H	H	*1b*
	F	F	F	F	F	*1c*
	F	H	F	H	H	*1d*
	H	Cl	H	H	H	*1e*
	H	H	Cl	H	H	*1f*
	H	H	Me	H	H	*1g*
	H	OMe	H	H	H	*1h*

Compounds **2**

R_1	R_2	R_3	R_4	R_5	R_6	
$N(Et)_2$	H	H	H	H	H	*2a*
	H	NO_2	H	H	H	*2b*
	F	F	F	F	F	*2c*
	F	H	F	H	H	*2d*
	H	Cl	H	H	H	*2e*
	H	H	Cl	H	H	*2f*
	F	H	H	H	F	*2g*
	H	H	F	H	H	*2h*
	H	H	Br	H	H	*2i*
	H	H	CHO	H	H	*2j*

Scheme 1

The present materials are all stable molecules obtained in high yields in easy one-step syntheses, by refluxing a stoichiometric amount of the appropriate salicylaldehyde with 2-amino-5-nitrophenol and the corresponding arylboronic acid in acetic acid.

Structure description

The molecular structure of **2a** is shown as an example in Fig. 1, but the structures of **2h** and **2i** (see ESI) reveal the same general trends as **2a**. At first, it seems that, except for the ethyl substituents of the amines and for the ArB– fragments, the organic skeletons are nearly planar, as expected in this family of substituted stilbene-based NLO chromophores. However, the stilbene skeletons are bent along the N–B bonds, which results in two planar N–(C_6H_4)(O)– donor and CH=N–(O)(C_6H_4)–NO_2 acceptor sub-units. The largest deviations from the mean planes, 0.133(4), 0.108(2), and 0.100(2) Å for **2a**, **2h**, and **2i**, respectively, are observed at O(4) in the donor units. Similarily, deviations of 0.114(1), 0.096(4), and 0.100(2) Å, respectively, are observed at C(7) in the acceptor units. The two planar sub-units are bent towards each other, as a result

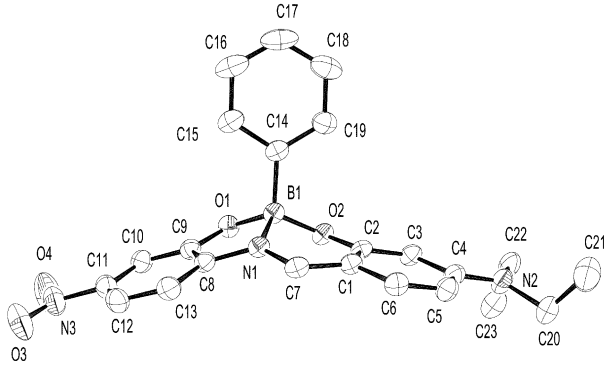

Fig. 1 Atom labeling scheme for **2a**. Hydrogen atoms are omitted for clarity.(Thermal ellipsoids at 30%.)

Table 1 Selected bond lengths (Å) and angles (°) (i) around the boron atom and (ii) in the C–C=N–C imine linkage for **2a**, **2h**, and **2i** (e.s.d.s. are in parentheses)

(i)	2a	2h	2i
O(1)–B(1)	1.494(2)	1.504(4)	1.493(7)
O(2)–B(1)	1.460(2)	1.463(4)	1.474(7)
B(1)–N(1)	1.586(2)	1.566(4)	1.580(7)
B(1)–C(14)	1.600(2)	1.609(5)	1.604(8)
O(1)–B(1)–O(2)	112.42(12)	111.1(2)	111.6(4)
O(2)–B(1)–C(14)	111.58(12)	111.9(2)	112.0(4)
O(1)–B(1)–C(14)	112.40(13)	112.2(3)	112.3(5)
O(1)–B(1)–N(1)	99.81(11)	100.2(2)	100.6(4)
O(2)–B(1)–N(1)	107.28(11)	108.7(3)	107.6(4)
N(1)–B(1)–C(14)	112.64(6)	112.2(2)	112.2 (4)

(ii)	2a	2h	2i
C(1)–C(7)	1.394(2)	1.390(4)	1.407(7)
C(7)–N(1)	1.3127(18)	1.324(4)	1.288(6)
N(1)–C(8)	1.3984(19)	1.397(3)	1.388(6)

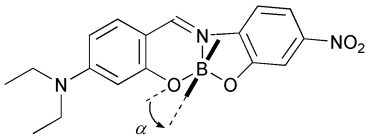

Scheme 2

of the tetrahedral geometry around the boron atom. This slight distortion leads to a reduction of the overlap along the π-conjugated pathway and, hence, is expected to reduce the NLO response *versus* that of related 4-diethylaminosalicylaldimine-based chromophores not containing boron.[22]

Bond lengths and angles associated with the tetrahedral geometry around the boron atom are listed in Table 1. The data reveals that changing the arylboron fragment does not significantly affect the coordination sphere around the boron atom. In particular, the magnitude of the length changes observed at the B(1)–N(1) bond, which might directly interfere with the charge transfer process, are modest and around 0.02 Å.

Finally, the most striking difference between the three molecular structures is observed in the relative orientation of the C(14)–C(19)-based phenyl moieties with respect to the stilbene backbone. Using the definition of the rotation angle (α) defined in Scheme 2, the crystal structure reveals α values of –11.3, +33.9, and +34.2° for **2a**, **2h**, and **2i**, respectively. These differences, which probably arise from different crystal environments, suggest a reduced potential barrier and, therefore, a possibility of easy rotation around the B(1)–C(14) bond.

Spectroscopic properties

The optical absorption spectra of **1a** and **2a**, recorded in chloroform are compared in Fig. 2. In both cases, the spectra are dominated by an intense band having absorption maxima at 461 (ε_{max} = 22 800) and 512 nm (ε_{max} = 63 900 $dm^3\ mol^{-1}\ cm^{-1}$) for **1a** and **2a**, respectively. A red shift and higher extinction coefficient observed on passing from **1a** to **2a** is consistent with the well-known electronic effect induced by using stronger donor–acceptor substituents on a stilbene backbone.[23] Additional transitions appear as shoulders in the spectra.

The spectroscopic features of derivatives **1** and **2** are gathered in Table 2. In most cases, the data reveal the presence of two transitions separated by about 20 nm, one of them being observed as a shoulder, usually at higher frequencies for **1** and lower frequencies for **2**. The intensity of the shoulder is usually more pronounced for **2**. A general tendency for red shifts

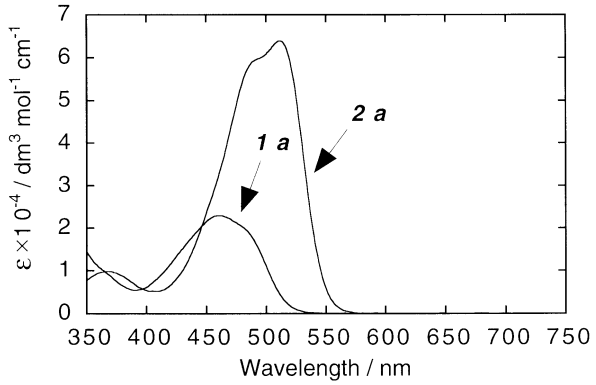

Fig. 2 Optical spectra of **1a** and **2a**, recorded in chloroform.

Table 2 Absorption maxima (in nm) and extinction coefficients (in dm^3 mol^{-1} cm^{-1}) from UV spectra of compounds **1** and **2** in chloroform

Compound	Transition 1	Transition 2
1a	461 (22 800)	475–485 (sh)
1b	457 (23 700)	470–480 (sh)
1c	446 (25 400)	465–475 (sh)
1d	451 (22 300)	
1e	459 (22 900)	470–480 (sh)
1f	458 (17 500)	475–485 (sh)
1h	460 (20 000)	480–490 (sh)
2a	490–500 (sh)	512 (63 900)
2b	485–495 (sh)	509 (50 900)
2c	475–485 (sh)	503 (48 200)
2d	481 (42 400)	495–505 (sh)
2e	485–495 (sh)	510 (46 800)
2f	441 (45 300)	
2g	485–495 (sh)	505 (54 600)
2h	485–495 (sh)	509 (50 700)
2i	485–495 (sh)	511 (53 800)
2j	446 (55 500)	505–515 (sh)

(around 50 nm) and roughly a doubling of the intensity on passing from **1** to **2** can be seen. For those of the Et_2N-based derivatives exhibiting the same qualitative spectra, a correlation can be found between the ^1H NMR shifts of the hydrogen atom of the imine (–HC=N) and the absorption maxima (λ_{max}), according to the graph shown in Fig. 3. The observation of an increase in the imine hydrogen NMR shift is consistent with an increase in the polarity of the C=N double bond, induced by the increasing withdrawing effect of the C(14)–C(19) fragment. This behavior, which is consistent with reduced charge transfer capabilities, reduced λ_{max} and β values, supports the initial idea

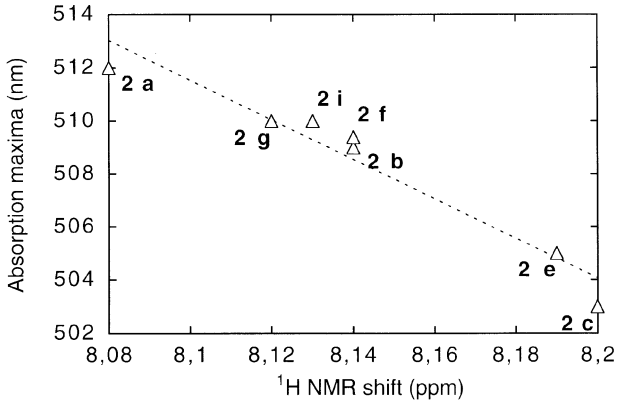

Fig. 3 ^1H NMR chemical shifts of H(7) as a function of the absorption maxima for compounds **2**.

Table 3 Powder SHG efficiencies (referenced to urea) for compounds **1** and **2** recorded at 1.907 μm

Compound	SHG
1a	0
1b	0
1c	0
1d	0.2
1e	0.3
1f	0.3
1g	0
1h	0.15
2a	0[a]
2b	0
2c	0
2d	0
2e	0
2f	0
2g	0
2h	0[a]
2i	0[a]
2j	0

[a]The crystal structures presented herein reveal that **2a** ($P2_1/c$), **2h** ($P2_1/a$), and **2i** ($P2_1/a$) crystallize in centrosymmetric space groups.

that changing the nature of the arylboron moiety has the potential to modulate the hyperpolarizability.

NLO properties

The powder SHG efficiencies of compounds **1** and **2** are listed in Table 3. Although derivatives **2** possess extended charge transfer capabilities in relation to the stronger donor strength of the Et_2N– groups, none of them exhibit a second harmonic signal. In contrast, half of the methoxy-based derivatives exhibit a modest, but non-zero, SHG powder efficiency. This seems to indicate a tendency for noncentrosymmetric space groups in compounds **1**, while all compounds **2** are likely to exist in centrosymmetric solid state environments.

The experimental hyperpolarizabilities of **1a** and **2a** measured by the electric field-induced second harmonic (EFISH) technique are shown in Table 4 and compared with the INDO calculated values. Although the agreement between calculation and experiment is not perfect, the data clearly reveal that β roughly doubles on passing from **1a** to **2a** at both the calculated and experimental levels.

It has long been recognized that the hyperpolarizabilities of donor–acceptor-substituted chromophores can be related to low-lying electronic transitions having charge transfer character, according to the following expression:[24]

$$\beta_{xxx} = \sum_i \frac{3e^2\hbar f \Delta\mu}{2m(\Delta E)^3} \times \frac{(\Delta E)^4}{\left((\Delta E)^2 - (2\hbar\omega)^2\right)\left((\Delta E)^2 - (\hbar\omega)^2\right)} \quad (1)$$

in which $\hbar\omega$ is the energy of the incident laser beam and β_{xxx} the principal tensor component along the charge transfer axis (x). 'Push–pull' stilbenes usually possess a dominant transition (i) of high intensity (oscillator strenth f), large dipole moment change ($\Delta\mu$), and low energy (ΔE), which accounts for most of the NLO response. According to this simplified, but widely used, two-level description, the red shift of 51 nm of the UV absorption maximum with increased intensity (from 22 800 to 63 900 dm^3 mol^{-1} cm^{-1}) observed on passing from **1a** to **2a**

Table 4 NLO data (β in 10^{-30} cm^{-5} esu^{-1} and μ in D) calculated by ZINDO and measured by EFISH for **1a** and **2a**

	1a		**2a**	
	β	μ	β	μ
Calculation	12.0	10.9	29.5	15.3
Experiment	27.0	10.2	46.4	13.6

Table 5 Experimental and calculated NLO response (β in 10^{-30} cm^{-5} esu^{-1} and μ in D) for fluorinated derivatives

	No. F atoms	Experimental (EFISH) data			Calculated (ZINDO) data		
		β_{vec}	μ	$\beta_{vec} \times \mu$	β	μ	$\beta \times \mu$
2a	0	45.0	14.0	630	28.8	15.3	441
2h	1	50.5	14.5	732	23.2	16.4	380
2g	2	48.0	16.0	768	28.0	16.0	448
2c	5	50.5	16.75	845	28.2	16.5	465

should lead to a β(**2a**) value equal to 4.2 times that of β(**1a**) at the experimental wavelength of 1.907 μm, a value that has to be compared to the experimental 1.7 times enhancement of the hyperpolarizability. The observation of a significant discrepancy can tentatively be related to the tetrahedral geometry of the boron derivatives, which could explain why a one-dimensional description of the charge transfer is not fully appropriate in the present case. Moreover, the fact that several components are involved in the intense bands, as evidenced in the UV-visible spectra, suggests that the NLO response arises from a set of several transition components, making the origin and magnitude of the effect difficult to fully rationalize within the framework of a simplified two-level model.

The possibilities for NLO property modulation induced by changing the electronic features of the arylboron fragment have been investigated on the basis of the various fluorine-substituted molecules available (**2a**, **2c**, **2g**, and **2h**). The overall molecular structures are grossly preserved within these substitutions. Therefore, the expected NLO modulations should likely arise from electronic rather than geometric modifications. A first examination of the UV-visible spectra (Table 2) reveals that increasing the attraction capabilities of the phenyl (by means of fluorination) results in a global trend for a blue shift of a few nanometers in the UV absorption maxima, and a reduction in the oscillator strength of about 20%, two effects that would lead to a lower β value, according to eqn. 1.

The experimental NLO responses are shown in Table 5, for the fluorinated derivatives. The data clearly reveal that the overall NLO response ($\beta \times \mu$) is slighly enlarged by fluorination, contrary to the two-level prediction. In fact, this effect arises from enhanced dipole moments, rather than from a modulation of the hyperpolarizabilities. Indeed, and within the approximations of both experimental and computational approaches, no clear effect on β is evidenced. Nevertheless, the over-simple two-level analysis is clearly not fully appropriate for the description of the NLO properties of this family of multi-dimensional charge transfer systems.

Finally, the observation of different possible orientations for the arylboron fragments in the solid state (see structure description) encouraged an investigation of the NLO consequences of potential easy rotations around the B(1)–C(14) bonds. The energy barrier associated with this behavior has been calculated for compound **2c** (Fig. 4). It is interesting to observe that for an energy cost of around 8 kcal, a rotation of about 40° leads to an enhancement of the hyperpolarizability equal to 30% of its initial value. This behavior may be related to the observation that the rotation process can result in short distances (2.4 to 2.5 Å) between the fluorine atoms and the stilbene backbone. This possibility, illustrated in Fig. 5, might modulate the overall electronic structure, the charge transfer process, and, hence, the hyperpolarizability.

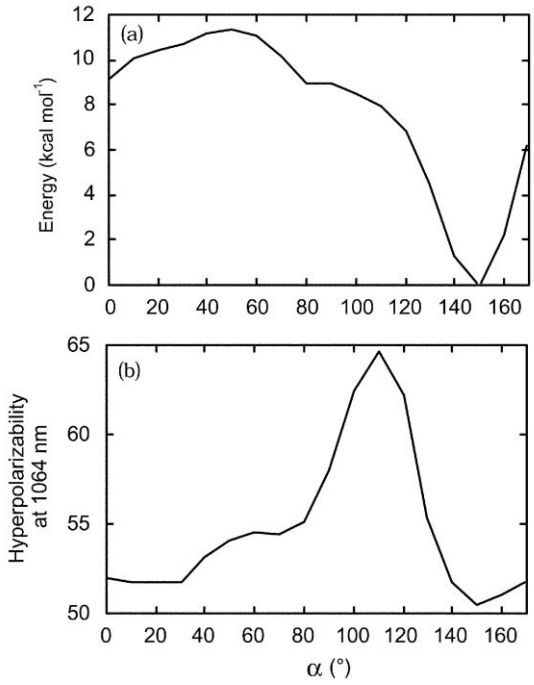

Fig. 4 Effect of rotation of the ArB– fragment on (a) the total molecular energy and (b) the hyperpolarizability, calculated at 1064 nm, for compound **2c**.

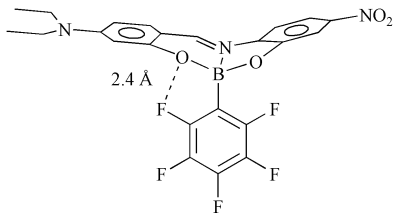

Fig. 5 Orientation which produces short (2.4 to 2.5 Å) F–O distances in compound **2c**. By comparison, the sum of the van der Waals radii for F–O is equal to 1.35 + 1.40 = 2.75 Å.

empty *p* orbitals in tricoordinate boron atoms as powerful π-acceptors;[25–27] (b) zwitterionic π-electron systems with boron and nitrogen charged groups at the end of the π-system, which offer an alternative to analogous push–pull compounds;[28] (c) acid–base adducts of pyridyl compounds with the Lewis acids BF_3 and $B(C_6F_5)_3$.[29]

In the present investigation, the introduction of an arylboron substituent leads to global reduction in β, arising from bent molecular geometry. The electronic effect on the hyperpolarizability induced through the highly polarized imine bond is found to be very modest. On the other hand, the results suggest that a significant NLO modulation could be achieved by rotation of the phenyl around the boron–carbon bond. Before being considered for a practical use, one might wonder how such a motion could be monitored. Using molecular rotors in operating devices has become an important issue of contemporary research in relation to the exciting concept of molecular machines.[30] To make such molecular devices work, energy has to be supplied in some way (*via* chemical, photochemical, or electrochemical reactions).[31] In the present case, the motion being an oscillation instead of a rotation, no external energy would have to be supplied, but a simple stimulus can be envisaged (*e.g.* an electric field pulse). Liquid crystalline materials and poled polymers could be possible candidates for this purpose. In particular, it has been observed that dipolar stilbenes incorporated into polymer matrices and submitted to intense electric fields remain tightly anchored into the polymer chains below the glass transition temperature, while substituted

A critical evaluation of the arylboron rotation for NLO purposes

In the field of molecular nonlinear optics, various boron-based materials have been reported to date. Basically, three different approaches were used in these systems: (a) the use of the

benzenes can retain some possibilities for rotation.[32] Reversible controls of these motions would probably be extremely difficult to achieve in an operative device. Nevertheless, nature has provided many examples of molecular motions occuring in hundreds of different biological molecular machines, each specialized for a particular function in different types of cells.[33] There is no reason to think that molecular engineering will not be able to reach this challenging target in the future.

Experimental

Materials and equipment

All starting materials were commercially available. Solvents were used without further purifications. Melting points were determined on a Gallenkamp MFB-595 apparatus and are uncorrected. NMR studies were performed on JEOL SX 270, JEOL Eclipse +400 and Bruker avance DPX 300 spectrometers. Chemical shifts (ppm) are relative to $(CH_3)_4Si$ for ^1H and ^{13}C and $BF_3{\cdot}OEt_2$ for ^{11}B. Coupling constants are quoted in Hz. UV spectra were obtained with a Perkin-Elmer Lambda 12 UV/VIS spectrophotometer. Mass spectra were recorded on a HP 5989A spectrometer. HMRS were collected on a JEOL 102A instrument.

Synthesis

The following procedure is representative for the preparation of all boron compounds described in this study. Equimolar amounts of 4-diethylaminosalicylaldehyde or 4-methoxysalicylaldehyde, 2-amino-5-nitrophenol and the corresponding arylboronic acid were refluxed in 10 ml of acetic acid for 3 h and cooled to room temperature. The solid precipitate was collected by filtration under vacuum and washed with small amounts of acetic acid. See ESI for details of the syntheses of compounds **1b**–**1h** and **2b**–**2j**.

2-Phenyl-(3′-nitrobenzo[*d*])-(4″-methoxybenzo[*h*])-1,3-dioxa-6-aza-2-boracyclonon-6-ene (**1a**) was prepared from 0.15 g (1.00 mmol) of 4-methoxysalicylaldehyde, 0.15 g (1.00 mmol) of 2-amino-5-nitrophenol and 0.12 g (1.00 mmol) of phenylboronic acid. The product was obtained as an orange solid (0.29 g, 0.77 mmol). Mp: 252–255 °C. Yield 77%. ^1H NMR (400 MHz, $CDCl_3$) [δ (ppm)]: 3.92 (3H, s, OCH_3), 6.59 (1H, dd, J = 8.8, 2.2 Hz, H-5), 6.67 (1H, d, J = 2.2 Hz, H-3), 7.14–7.21 (3H, m, H-16, H-17, H-18), 7.29-7.31 (2H, m, H-15, H-19), 7.35 (1H, d, J = 8.8 Hz, H-6), 7.46 (1H, d, J = 8.8 Hz, H-13), 7.83 (1H, dd, J = 8.8, 2.2 Hz, H-12), 7.88 (1H, d, J = 2.2 Hz, H-10), 8.39 (1H, s, H-7) (the atom numbering scheme for the NMR data refers to Fig. 1); ^{11}B NMR (128.2 MHz, $CDCl_3$) [δ (ppm)]: 8.3 ($h_{1/2}$ = 285 Hz). MS (EI, 15 eV): *m*/*z* 374 (M^+, 8), 297 (100), 267 (13), 251 (23). HRMS calcd for $C_{20}H_{15}O_5N_2B$: 374.1074; found 374.1093.

2-Phenyl-(3′-nitrobenzo[*d*])-(4″-diethylaminobenzo[*h*])-1,3-dioxa-6-aza-2-boracyclonon-6-ene (**2a**) was prepared from 0.19 g (1.00 mmol) of 4-diethylaminosalicylaldehyde 0.15 g (1.00 mmol) of 2-amino-5-nitrophenol and 0.12 g (1.00 mmol) of phenylboronic acid. The product was obtained as a red solid (0.39 g, 0.93 mmol). Mp: 212–214 °C. Yield 93%. ^1H NMR (270 MHz, $CDCl_3$) [δ (ppm)]: 1.24 (6H, t, J = 7.1, CH_3), 3.46 (4H, m, NCH_2), 6.35 (1H, dd, J = 8.4, 2.4 Hz, H-5), 6.32 (1H, d, J = 2.4 Hz, H-3), 7.14–7.17 (4H, m, H-6, H-16, H-17, H-18), 7.23 (1H, d, J = 8.4 Hz, H-13), 7.33-7.36 (2H, m, H-15, H-19), 7.73 (1H, dd, J = 8.4, 2.2 Hz, H-12), 7.77 (1H, d, J = 2.2 Hz, H-10), 8.08 (1H, s, H-7); ^{13}C NMR (67.9 MHz, $CDCl_3$) [δ (ppm)]: 12.80 (CH_3), 45.41 (NCH_2), 99.10 (C-3), 107.63 (C-5), 108.88 (C-10), 110.30 (C-1), 112.33 (C-13), 115.33 (C-12), 127.51 (C-16), 127.81 (C-17), 130.99 (C-15), 134.44 (C-6), 138.19 (C-11), 147.40 (C-8), 148.40 (C-7), 157.06 (C-9), 157.36 (C-4), 161.04 (C-2); ^{11}B NMR (128.2 MHz, $CDCl_3$) [δ (ppm)]: 8.5 ($h_{1/2}$ = 139 Hz). MS (EI, 15 eV): *m*/*z* 415 (M^+, 12), 338 (100), 308 (22), 292 (30). HRMS calcd for $C_{23}H_{22}O_4N_3B$: 415.1703; found 415.1702.

Table 6 Crystal data for **2a**, **2h**, and **2i**

	2a	**2h**	**2i**
Chemical formula	$C_{23}H_{22}BN_3O_4$	$C_{23}H_{21}BFN_3O_4$	$C_{23}H_{21}BBrN_3O_4$
Formula weight	415.25	433.24	494.15
Crystal system	Monoclinic	Monoclinic	Monoclinic
Space group	$P2_1/c$	$P2_1/a$	$P2_1/a$
a/Å	11.1674(4)	11.229(4)	11.27(3)
b/Å	7.7630(3)	15.668(5)	16.565(9)
c/Å	24.1683(9)	12.587(4)	12.270(12)
β/°	90.7300(10)	108.23(1)	107.45(4)
V/Å^3	2095.04(14)	2103.4(6)	2185(6)
Temperature/K	293(2)	293(2)	293(2)
Z	4	4	4
Collected reflections	13417	4460	4050
Independent reflections	4136	4237	3843
R^a	0.0441	0.0466	0.0431
$R_w{}^b$	0.1154	0.1158	0.1112
Variables	283	362	373

$^aR = \Sigma\|F_o| - |F_c\|/\Sigma|F_o|$. $^bR_w(F_o)^2 = [\Sigma_w(F_o^2 - F_c^2)^2/\Sigma_w F_o^4]^{1/2}$

X-Ray data collection and structure determination

X-Ray diffraction studies were carried out using Enraf Nonius-CAD4 and Bruker AXS Smart 600 diffractometers with CCD scan-type hemispheres ($\lambda_{Mo\text{-}K\alpha}$ = 0.71073 Å, graphite monochromator, T = 293 K, $\omega/2\theta$ scan mode) the crystals were mounted in LINDEMAN tubes. Absorption corrections were performed using the SHELX-A procedure,[34] corrections were made for Lorentz and polarization effects. Solution and refinement: direct methods, SHELX-S-97 for structure solution and SHELX-L-97 ver. 34 for refinement and data output[34] applied in the WIN-GX program set;[35] the corresponding images were prepared with ORTEP 3.[36] Hydrogen atoms were located on difference Fourier maps and their positions systematically modeled and calculated, followed by one overall isotopic thermal parameter refinement. The non-hydrogen atoms were refined anisotropically. Crystallographic data for **2a**, **2h**, and **2i** are summarized in Table 6.

CCDC reference numbers 175921–175923.

See http://www.rsc.org/suppdata/jm/b2/b205308j/ for crystallographic data in CIF or other electronic format.

Theoretical methods

The INDO/1 method,[37] in connection with the sum-over-state (SOS) formalism,[38] was employed for the calculation of the molecular hyperpolarizabilities of **2a** and **2h** using the set of coordinates available from the crystal structures. In the case of **1a**, **2c**, and **2g**, the metrical parameters were taken from the crystal structure of the related **2a** compound, with standard C–F distances equal to 1.38 Å, and standard O–C distances equal to 1.43 Å (MeOAr– fragment of **1a**). Details for the computationally efficient INDO-SOS-based method for describing second-order molecular nonlinearities have been reported elsewhere.[39] The calculation of the electronic transitions and molecular hyperpolarizabilities was performed using the commercially available MSI software package INSIGHT II (4.0.0).[40] The close-shell restricted Hartree–Fock (RHF) formalism was employed. The mono-excited excitation interaction (MECI) approximation was used to describe the excited states. The 100 energy transitions between the ten highest occupied molecular orbitals and the ten lowest unoccupied ones were chosen to undergo CI mixing. The calculation of the rotation barrier for compound **2c** was performed by using INDO/1. For each calculation, the molecular geometry was fixed, whereas the dihedral angle (α, Scheme 2) was varied from 0 to 180° in 10° steps.

NLO measurements

Second harmonic generation (SHG) measurements were carried out by the Kurtz–Perry powder test,[41] using a nanosecond-pulsed Nd-YAG (10 Hz) laser. The fundamental beam (1.064 μm) was focused in a hydrogen cell (1 m long, 50 atm.) and the outcoming Stokes-shifted radiation at 1.907 μm used as the fundamental beam for SHG. The second harmonic signal was detected by a photomultiplier and read on an ultrafast Tektronic TDS 620B oscilloscope. Samples were uncalibrated microcrystalline powders obtained by grinding and put between two glass plates. β Measurements were carried out by the electric field-induced second harmonic (EFISH) technique.[42,43] The compounds were dissolved in chloroform at various concentrations (0 to 2×10^{-2} mol L^{-1}), and the centrosymmetry of the solution was broken by high voltage pulses of 5 kV synchronized with the laser pulse. Further details of the EFISH methodology and data analysis are reported elsewhere.[43]

The NLO response being induced by dipolar orientation of the chromophores, the NLO response is proportionnal to $\mu \times \beta_{vec}$, (μ being the dipole moment and β_{vec} the vector component of β along the dipole moment direction). μ Values were measured independently by a classical method based on the Guggenheim theory.[44] Although μ and β are probably not strictly parallel, the comparisons between experimental and calculated hyperpolarizabilities are based on the assumption that comparing β_{vec} values is the same as comparing β values.

Acknowledgements

The authors acknowledge Jean-François Delouis for his help with the EFISH measurements and Consejo Nacional de Ciencia y Teconologia (CONACYT, Mexico) for financial support.

References

1 (*a*) *Introduction to Nonlinear Optical Effects in Molecules and Polymers*, ed. P. N. Prasad and D. J. Williams, Wiley, New York, 1991; (*b*) *Nonlinear Optical Materials*, ed. H. Kuhn and J. Robillard, CRC Press, Boca Raton, 1992; (*c*) *Nonlinear Optics of Organic Molecules and Polymers*, ed. H. S. Nalwa and S. Miyata, CRS Press, New York, 1997.
2 (*a*) T. Verbiest, S. Houbrechts, M. Kauranen, K. Clays and A. Persoons, *J. Mater. Chem.*, 1997, **7**, 2175; (*b*) L. R. Dalton, A. W. Harper, R. Ghosn, W. H. Steier, M. Ziari, H. Fetterman, Y. Shi, R. V. Mustacich, A. K. Y. Jen and K. J. Shea, *Chem. Mater.*, 1995, **7**, 1060.
3 *Optical Nonlinearities in Chemistry*, special issue of *Chem. Rev.,* 1994, **94**.
4 C. Chen and G. Liu, *Annu. Rev. Mater. Sci.*, 1986, **16**, 203.
5 *NonlinearOptical Properties of Organic Molecules and Crystals*, ed. D. S. Chemla and J. Zyss, Academic Press, New York, 1987.
6 (*a*) S. R. Marder, D. N. Beratan and L. T. Cheng, *Science*, 1991, **252**, 103; (*b*) S. R. Marder, C. B. Gorman, B. G. Tiemann and L. T. Cheng, *J. Am. Chem. Soc.*, 1993, **115**, 3006.
7 J. M. Lehn, *Supramolecular Chemistry—Concepts and Perspectives*, VCH, Weinheim, 1995.
8 (*a*) M. D. Ward, *Chem. Soc. Rev.*, 1995, **24**, 121; (*b*) J. A. Delaire and K. Nakatani, *Chem. Rev.*, 2000, **100**, 1817.
9 See, for instance: (*a*) B. J. Coe, *Chem. Eur. J.*, 1999, **5**, 2464; (*b*) M. Malaun, Z. R. Reeves, R. L. Paul, J. C. Jeffery, J. A. McCleverty, M. D. Ward, I. Asselberghs and A. Persoons, *Chem. Commun.*, 2001, 49.
10 S. Houbrechts, K. Clays, A. Persoons, Z. Pikramenou and J. M. Lehn, *Chem. Phys. Lett.*, 1996, **258**, 485.
11 K. Nakatani and J. A. Delaire, *Chem. Mater.*, 1997, **9**, 2682.
12 B. J. Coe, S. Houbrechts, I. Asselberghs and A. Persoons, *Angew. Chem., Int. Ed.*, 1999, **38**, 366.
13 R. Loucif-Saïbi, K. Nakatani, J. A. Delaire, M. Dumont and Z. Sekkat, *Chem. Mater.*, 1993, **5**, 229.
14 S. L. Gilat, S. H. Kawai and J. M. Lehn, *Chem. Eur. J.*, 1995, **1**, 275.
15 (*a*) M. T. Reetz, C. M. Niemeyer and K. Harms, *Angew. Chem., Int. Ed. Engl.*, 1991, **30**, 1472; (*b*) M. T. Reetz, C. M. Niemeyer and K. Harms, *Angew. Chem., Int. Ed. Engl.*, 1991, **30**, 1474.
16 K. Worm, F. P. Schmidtchem, A. Schier, A. Schäfer and M. Hesse, *Angew. Chem., Int. Ed. Engl.*, 1994, **33**, 327.
17 E. Graf, M. W. Hosseini, A. De Cian and J. Fischer, *Bull. Soc. Chim. Fr.*, 1996, **133**, 743.
18 T. D. James, K. R. A. Samankumara Sandanayake and S. Shinkai, *Angew. Chem., Int. Ed. Engl.*, 1996, **35**, 1910.
19 V. Barba, Ph.D. Thesis, CINVESTAV, Mexico, 2001.
20 (*a*) N. Farfán, R. Santillan and H. Höpl, *Main Group Chem. News*, 2000, **7**, 3; (*b*) V. Barba, R. Luna, D. Castillo, R. Santillan and N. Farfán, *J. Organomet. Chem.*, 2000, **604**, 273; (*c*) N. Farfán, H. Höpl, V. Barba, M. E. Ochoa, R. Santillan, E. Gómez and A. GutiÈrrez, *J. Organomet. Chem.*, 1999, **581**, 70; (*d*) F. Höpl, M. Sanchez, N. Farfán, S. Rojas and R. Santillan, *Inorg. Chem.*, 1998, **37**, 1679; (*e*) V. Barba, E. Gallegos, R. Santillan and N. Farfán, *J. Organomet. Chem.*, 2001, **622**, 259.
21 (*a*) H. Höpl, M. Sanchez, N. Farfán and V. Barba, *Can. J. Chem.*, 1998, **76**, 1352; (*b*) V. Barba, D. Cuahutle, R. Santillan and N. Farfán, *Can. J. Chem.*, 2001, **79**, 1229.
22 P. G. Lacroix, F. Averseng, I. Malfant and K. Nakatani, unpublished results.
23 L. T. Cheng, W. Tam, S. R. Marder, A. E. Stiegman, G. Rikken and C. W. Sprangler, *J. Phys. Chem.*, 1991, **95**, 10 643.
24 J. L. Oudar, *J. Chem. Phys.*, 1977, **67**, 446.
25 C. Branger, M. Lequan, R. M. Lequan, M. Barkazoukas and A. Fort, *J. Mater. Chem.*, 1996, **6**, 555.
26 Z. Yuang, N. J. Taylor, T. B. Marder, I. D. Williams, S. K. Kurtz and L. T. Cheng, *J. Chem. Soc., Chem. Commun.*, 1990, 1489.
27 L. Bosio, R. M. Lequan, M. Lequan and M. Vandevyver, *New J. Chem.*, 1995, **19**, 141.
28 C. Lambert, S. Stadler, G. Bourhill and C. Brauchle, *Angew. Chem., Int. Ed. Engl.*, 1996, **35**, 644.
29 M. J. Gerald, A. Woodward, N. J. Taylor, T. B. Marder, I. Cazenobe, I. Ledoux, J. Zyss, A. Thornton, D. W. Bruce and A. K. Kakkar, *Chem. Mater.*, 1998, **10**, 1355.
30 *Molecular Machines*, special issue of *Acc. Chem. Res.* 2001, **34**(6).
31 R. Ballardini, V. Balzani, A. Credi, M. T. Gandolfi and M. Venturi, *Acc. Chem. Res.*, 2001, **34**, 445.
32 See, for instance: (*a*) M. Dumont, Z. Sekkat, R. Loucif-Saïbi, K. Nakatani and J. A Delaire, *Nonlinear Opt.*, 1993, **5**, 395; (*b*) E. Ishow, L. Qiu, J. A. Delaire and K. Nakatani, *Pure Appl. Opt.*, 2002, in press.
33 R. D. Vale and R. A. Milligan, *Science*, 2000, **288**, 88.
34 G. M. Sheldrick, SHELX97, Programs for Crystal Structure Solution and Refinement, University of Göttingen, Germany, 1997.
35 L. J. Farrugia, *J. Appl. Crystallogr.*, 1999, **32**, 837.
36 ORTEP 3L. J. Farrugia, *J. Appl. Crystallogr.*, 1997, **30**, 837.
37 (*a*) M. C. Zerner, G. Loew, R. Kirchner and U. Mueller-Westerhoff, *J. Am. Chem. Soc.*, 1980, **102**, 589; (*b*) W. P. Anderson, D. Edwards and M. C. Zerner, *Inorg. Chem.*, 1986, **25**, 2728.
38 J. F. Ward, *Rev. Mod. Phys.*, 1965, **37**, 1.
39 (*a*) D. R. Kanis, T. J. Marks and M. A. Ratner, *Int. J. Quantum Chem.*, 1992, **43**, 61; (*b*) D. R. Kanis, M. A. Ratner and T. J. Marks, *Chem. Rev.*, 1994, **94**, 195.
40 M. J. Frisch, G. W. Trucks, H. B. Schlegel, P. M. W. Gill, B. G. Johnson, M. A. Robb, J. R. Cheeseman, T. Keith, G. A. Petersson, J. A. Montgomery, K. Raghavachari, M. A. Al-Laham, V. G. Zakrzewski, J. V. Ortiz, J. B. Foresman, J. Cioslowski, B. B. Stefanov, A. Nanayakkara, M. Challacombe, C. Y. Peng, P. Y. Ayala, W. Chen, M. W. Wong, J. L. Andres, E. S. Replogle, R. Gomperts, R. L. Martin, D. J. Fox, J. S. Binkley, D. J. Defrees, J. Baker, J. P. Stewart, M. Head-Gordon, C. Gonzalez and J. A. Pople, Gaussian 94, Revision E2, Gaussian, Inc., Pittsburgh, PA, USA, 1995.
41 (*a*) S. K. Kurtz and T. T. Perry, *J. Appl. Phys.*, 1968, **39**, 3798; (*b*) J. P. Dougherty and S. K. Kurtz, *J. Appl. Crystallogr.*, 1976, **9**, 145.
42 (*a*) J. L. Oudar, *Chem. Phys.*, 1977, **67**, 446; (*b*) B. F. Levine and C. G. Betha, *J. Chem. Phys.*, 1975, **63**, 2666; (*c*) B. F. Levine and C. G. Betha, *J. Chem. Phys.*, 1976, **65**, 1989.
43 I. Maltey, J. A. Delaire, K. Nakatani, P. Wang, X. Shi and S. Wu, *Adv. Mater. Opt. Electron.*, 1996, **6**, 233.
44 E. A. Guggenheim, *Trans. Faraday Soc.*, 1949, **45**, 714.